Transcriptome profile of polycyclic aromatic hydrocarbon-degrading fungi isolated from *Taxus* rhizosphere

Rui Gao[1,$], Da Cheng Hao[1,*,$], Wenli Hu[1], Song Song[1], Shi Yang Li[2] and Guang Bo Ge[2,3]

[1]School of Environment and Chemical Engineering, Dalian Jiaotong University, Dalian 116028, China
[2]Laboratory of Pharmaceutical Resource Discovery, Dalian Institute of Chemical Physics, Chinese Academy of Sciences, Dalian 116023, China
[3]Institute of Interdisciplinary Medicine, Shanghai University of Traditional Chinese Medicine, Shanghai 201203, China

The present study aims to examine polycyclic aromatic hydrocarbon (PAH)-degrading fungal strains isolated from rhizosphere soil of *Taxus mairei*. *Talaromyces verruculosus* strain DJTU-SJ5 showed the higher PAH degradation than other strains. Improved degradation of five PAHs was attained using the two-member consortium. The industrial potential of DJTU-SJ5 has been highlighted. The transcriptome profiles of DJTU-SJ5 before and after PAH challenge were decoded by high-throughput RNA sequencing. A total of 33,084 unigenes were obtained by *de novo* assembly of 19.9 Gb clean sequencing reads; 10,532, 1,104 and 11,779 unigenes were expressed distinctly between control and phenanthrene (phen)-treated samples; control and pyrene (pyre)-treated samples, and phen and pyre respectively. These included numerous PAH degradation, defence and stress-related genes. The degradation pathway of PAHs in strain DJTU-SJ5 is proposed based on the metabolites and transcriptome analyses.

Keywords: Biodegradation, polycyclic aromatic hydrocarbon, *Talaromyces verruculosus*, *Taxus mairei*, transcriptome sequencing.

BIOPROSPECTING of bioactive catalysts and molecules from plants and microbes has attracted much attention in building a sustainable bio-economy. Polycyclic aromatic hydrocarbons (PAHs), such as low molecular weight PAHs (e.g. naphthalene, acenaphthene and phenanthrene) and the highly recalcitrant high molecular weight PAHs (pyrene and benzo[a]pyrene (BaP)), are globally distributed in wastewater, solid waste and polluted soil. PAH-degrading fungi are useful in many industrial settings, e.g. wastewater treatment, biomass transformation[1] and soil bioremediation. The striking microbial diversity of *Taxus* rhizosphere has been revealed by shotgun metagenomic sequencing[2]. Though the rhizosphere, which is rich in PAH-degrading fungi, awaits further studies, no such strains from *Taxus* rhizosphere have been reported till now.

*For correspondence. (e-mail: hao@djtu.edu.cn)
$Contributed equally to this work.

Talaromyces, a genus of Ascomycota, has versatile utility in biotransformation and pollutant removal. For example, *Talaromyces verruculosus* SGMNPf3 is able to release secretory enzymes during cellulosic biomass degradation[3]. *Talaromyces trachyspermus* OU5 was isolated from soil and could produce rich exopolymers that have excellent flocculation ability to deal with kaolin suspension and swine wastewater[4]. *Abortiporus biennis* has long been known as a white-rot fungus[5], which can detoxify and decolourize effluents from the green olive debittering process. *A. biennis* is also useful in cadmium sequestration[6] and phenolic degradation[7]. However, studies regarding the use of *Talaromyces* and *Abortiporus* in organic pollutant removal and bioremediation are still limited. Cell type-specific gene expression alterations of the dimorphic pathogen *Talaromyces marneffei* was characterized using the microarray approach[8]. Transcriptome sequencing of *Talaromyces marneffei* was used to study mechanisms of environmental adaptation and virulence[9]. However, the PAH degradation mechanisms of *Talaromyces* have not been studied using the transcriptome sequencing approach. Strains with various biotransformation potential have been isolated from *Taxus* (the source plant of the anticancer taxanes) rhizosphere[10,11], which prompted us to utilize the powerful omics tool for further probing the functional capability of *Taxus* rhizosphere microbiome.

In this study, we characterized three PAH-degrading fungi, including a novel *Talaromyces verruculosus* strain DJTU-SJ5, from the rhizosphere soil of *Taxus mairei*, an endangered gymnosperm species of southern China. The medium composition of DJTU-SJ5 for maximal PAH degradation was improved by single-factor experiments and statistically based experimental design. The PAH degradation and dye-deletion performance of DJTU-SJ5 and/or DJTU-SJ5-containing consortium were characterized to ascertain their industrial potential. Transcriptome profiles of DJTU-SJ5, obtained using the high-throughput Illumina sequencing and *de novo* unigene assembly, were compared before and after PAH treatments, which contribute information for mechanism studies of PAH degradation.

Materials and methods

Quantifying PAH degradation

The seed medium (beef extract 3 g, peptone 10 g, NaCl 4 g, 1 litre) was used to grow PAH-degrading fungi at 25°C and 130 rpm for 48 h. Then the culture suspension was centrifuged at 6000 rpm for 5 min, and phosphate buffer was used to wash the pellet thrice. Five millilitre cell suspension was made for the degradation tests. The 50 ml reaction mixture consisted of 2 ml fourfold concentrated fungal suspension, 300 mg/l Tween 80, PAH (phenanthrene, final concentration 150 mg/l; pyrene, 95 mg/l; acenaphthene, 200 mg/l; naphthalene, 200 mg/l; BaP, 20 mg/l) and inorganic salt media. In the two-member consortium, 1 ml of each fungal suspension was added in the reaction mixture. Every test was performed in triplicate at 30°C, 150 rpm for one week. The reaction mixture was centrifuged at 6000 rpm for 25 min to get the supernatant. The degradation products were extracted from the filtered supernatant by C18 solid phase microextraction column (Agilent, China), and dichloromethane was used as the elution solvent with elution rate of 2 ml/min. The non-degraded PAH substrate was determined based on UV absorbance of 289 nm (phenanthrene), 252 nm (pyrene), 309 nm (acenaphthene), 283 nm (naphthalene) or 295 nm (BaP). The percentage of PAH degradation was determined by standard curves.

In mixed PAH degradation, 50 mg/l pyrene, 100 mg/l phenanthrene, 100 mg/l naphthalene, 100 mg/l acenaphthene and/or 20 mg/l (100 mg/l in ternary and penternary mixtures) BaP were used in various combinations. Chemical oxygen demand (COD) was determined by the standard potassium dichromate method. Every experiment was repeated thrice at 30°C and 150 rpm for 24 h or 5 d.

Chromatography (HPLC) and spectrometry (MS)

The degradation mixture was centrifuged and degradation products were extracted from the filtered supernatant. The extract was then vacuum-dried. The solid residue was dissolved in 2 ml HPLC-grade acetonitrile as the trial sample. PAH (95 mg/l pyrene, 150 mg/l phenanthrene, 200 mg/l naphthalene or acenaphthene, or 20 mg/l BaP) was used as control. LC-10ATvp (Shimadzu, Japan) HPLC system was used with the following parameters: C18 column, 250 × 4.6 × 5 µm, 30°C, injection volume 10 µl, flow rate 1 ml/min, mobile phase H_2O/acetonitrile, detection wavelength 242 nm; gradient elution: 0–10 min, H_2O 40%/acetonitrile 60%; 10–12 min, H_2O 15%/acetonitrile 85%; 12–18 min, H_2O 10%/acetonitrile 90%; 18–23 min, H_2O 40%/acetonitrile 60%.

LC-MS-2010EV (Shimadzu, Japan) was used to infer the PAH metabolites via fungal strains with the following conditions: C18 column, 250 × 2.1 × 5 µm, 30°C, injection volume 5 µl, flow rate 0.4 ml/min, mobile phase H_2O/acetonitrile, detection wavelength 232 nm; gradient elution: 0–2 min, H_2O 90%/acetonitrile 10%; 2–8 min, H_2O 70%/acetonitrile 30%; 8–11 min, H_2O 6%/acetonitrile 94%; 11–12 min, H_2O 5%/acetonitrile 95%; 12–15 min, H_2O 90%/acetonitrile 10%).

RNA extraction

The single colony of *Talaromyces verruculosus* was inoculated into three 500 ml flasks containing sucrose 2 g, peptone 1 g, KH_2PO_4 0.2 g, $MgSO_4$ 0.05 g, $CaCl_2$ 0.0075 g, $CuSO_4$ 0.001 g and H_2O 100 ml; the control culture without PAH was named 'ordi'. The single colony from the same culture dish was put into three 500 ml flasks of the ordinary medium plus 100 mg/l phenanthrene (named 'phen'). Similarly, the single colony was put in the ordinary medium plus 100 mg/l pyrene (named 'pyre'). Fungi were grown in the shaking flask culture at 25°C for five days; then fresh media of the same components were supplemented into the flasks. RNA of fungal mycelia was extracted after 24 h of culture. TRIzol reagent was used to extract the total RNA from *Talaromyces verruculosus*. The total RNA from three technical replicates of ordi was mixed equally, and RNA mixture was obtained from phen and pyre respectively. The highly pure RNA was used in transcriptome profiling.

Transcriptome profiling and bioinformatics

The high-throughput sequencing libraries of ordi, phen and pyre were constructed as described previously[12]. By base calling, the original image data for three groups (control, phenanthrene and pyrene treatments) generated by the Illumina HiSeq 4000 sequencer were converted into raw reads, available at NCBI SRA (accession nos. SRR5760131, SRR5760132 and SRR5760133 respectively). Trinity (http://trinityrnaseq.sourceforge.net/) was used in the *de novo* sequence assembly of clean reads. The clean reads (ordi 50,128,308, phen 45,047,260 and pyre 44,118,522) were mapped to the assembled unigenes to analyse differentially expressed genes (DEGs). FPKM (fragments per kb of exon per million fragments mapped) was adopted to represent unigene expression levels.

The open reading frame (ORF) was predicted by Trinity. Pfam database (http://pfam.sanger.ac.uk) and HMMER3 program were used to analyse the protein domain and gene family. The unigene annotations were performed by the alignments of NCBI NR, String, Swissprot, COG and KEGG databases with BlastX. The functional annotations of biological process, molecular function and cellular component were performed using BLAST2GO and the GO database.

The DEG analysis was performed using the software edgeR (http://www.bioconductor.org/packages/2.12/bioc/

html/edgeR.html). The significance of gene expression difference was judged using FDR (false discovery rate) ≤ 0.05 and the absolute value of $\log_2$(fold change) ≥ 1. Clusters of gene expression patterns were analysed as described previously[12]. DEGs were subjected to the GO classification and KEGG pathway visualization. The software Goatools (https://github.com/tanghaibao/GOatools) was used to perform the GO enrichment analysis and provide GO terms substantially enriched in DEGs. The calculated *P*-value underwent Bonferroni correction, and the corrected *P*-value ≤ 0.05 was considered significant. The GO-directed acyclic graphs were drawn to display the hierarchical structure of the enriched GO terms. Moreover, the dramatically enriched metabolic pathways in DEGs were found by the pathway enrichment analysis.

Results and discussion

Fungal strains and ITS identification

The PAH-degrading fungi, i.e. *Talaromyces verruculosus* (Eurotiomycetes) strain DJTU-SJ5, an *A. biennis* (Agaricomycetes, Basidiomycota) strain and a *Fusarium oxysporum* (Sordariomycetes) strain, were isolated from *T. mairei* rhizosphere[13]. The NCBI GenBank accession numbers of *F. oxysporum* ITS, *T. verruculosus* ITS and *A. biennis* ITS are MG760439, MG760440 and MG760441 respectively. DJTU-SJ5 and *Fusarium* belong to Ascomycota, while *Abortiporus* belongs to Basidiomycota. The PAH-degrading activities of different *F. oxysporum* strains varied greatly[14], the *Fusarium* strain isolated in this study could not survive with more than 50 mg/l pyrene, while the other two strains grew well with 200 mg/l pyrene.

Based on the single factor experiments and uniform design, the optimal medium for PAH degradation contained, pyrene 95 mg/l, phenanthrene 150 mg/l, naphthalene 200 mg/l or acenaphthene 200 mg/l and 300 mg/l Tween 80 at pH 6.0. Three replicate experiments using this optimized medium composition yielded an average 83.2% (pyrene), 92.38% (phenanthrene), 96.88% (acenaphthene), 99.51% (naphthalene) and 60.0% (BaP 100 mg/l) degradation via DJTU-SJ5. The cellulolytic characteristics of *T. verruculosus* has been reported[3], but *T. verruculosus* strain with PAH degradation ability has not been characterized. Our results suggested this fungus as a potential PAH degrader which could be useful in wastewater treatment and bioremediation.

PAH degradation

In the whole-cell transformation, all five PAHs were efficiently degraded by DJTU-SJ5 within seven days[13]; the two-ring PAH naphthalene was best degraded (99.51% ± 1.06%), and the degradation percentage of three-ring PAHs was 92.38 ± 0.73 (phenanthrene) and 96.88 ± 0.15 (acenaphthene) respectively. The four-ring PAH pyrene was also well degraded (83.2% ± 1.46%). DJTU-SJ5 degraded 60% five-ring PAH BaP, known for its recalcitrance. The original, benzene and naphthalene derivatives can be transformed by the immobilized *A. biennis* to non-toxic products[15]. The *A. bortiporus* strain isolated in our previous study could transform two-ring and three-ring PAHs[13], but it is weak in transforming four- and five-ring PAHs. Many fungal strains participate in PAH degradation in the environment[1]. In the present study more complete removal of two- and three-ring PAHs by DJTU-SJ5 + *A. bortiporus* was observed (Figure 1), and pyrene degradation was significantly improved using the fungal consortium, implying cooperation between two fungi.

When pyrene was used as the sole substrate, within 24 h DJTU-SJ5 and *A. biennis* degraded 77.65% and 62.12% pyrene respectively (Figure 2 *a*). When phenanthrene or naphthalene was involved in the pyrene-containing binary mixture, pyrene degradation via DJTU-SJ5 was enhanced, which was otherwise decreased by acenaphthene. Similarly, pyrene degradation via *A. biennis* was decreased by phenanthrene, illustrating the substrate competition commonly found among PAH-degrading microbes[1]. The inhibition of phenanthrene degradation via both strains by the highly toxic pyrene (Figure 2 *b*), the reduction of acenaphthene degradation by pyrene (Figure 2 *c*), as well as BaP inhibition of pyrene degradation via DJTU-SJ5, *F. oxysporum* or their combination (Figure 2 *d*), provide more examples of competitive inhibition. *F. oxysporum*-containing consortium was able to degrade and mineralize 250–1000 mg/kg phenanthrene and pyrene in soil[16], signifying the synergistic promotion of PAH mineralization by mixtures of

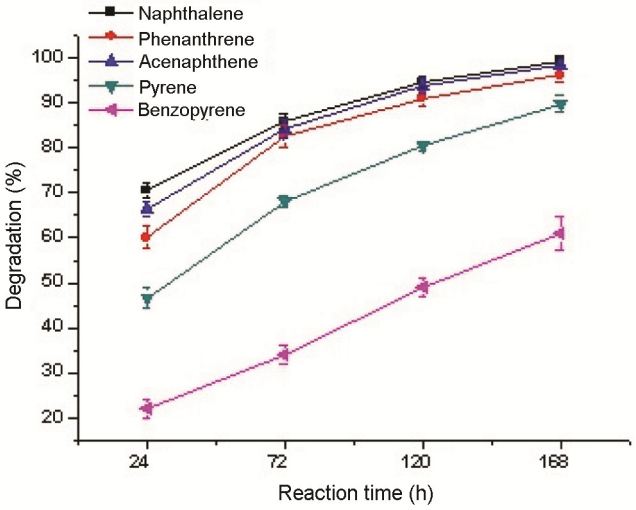

Figure 1. Polycyclic aromatic hydrocarbon (PAH) degradation by fungal strain DJTU-SJ5 + *Abortiporus biennis* isolated from *Taxus mairei*. The final concentration of pyrene, phenanthrene, naphthalene, acenaphthene and benzopyrene was 95, 150, 200, 200 and 20 mg/l respectively. Error bars are standard deviations (n = 3).

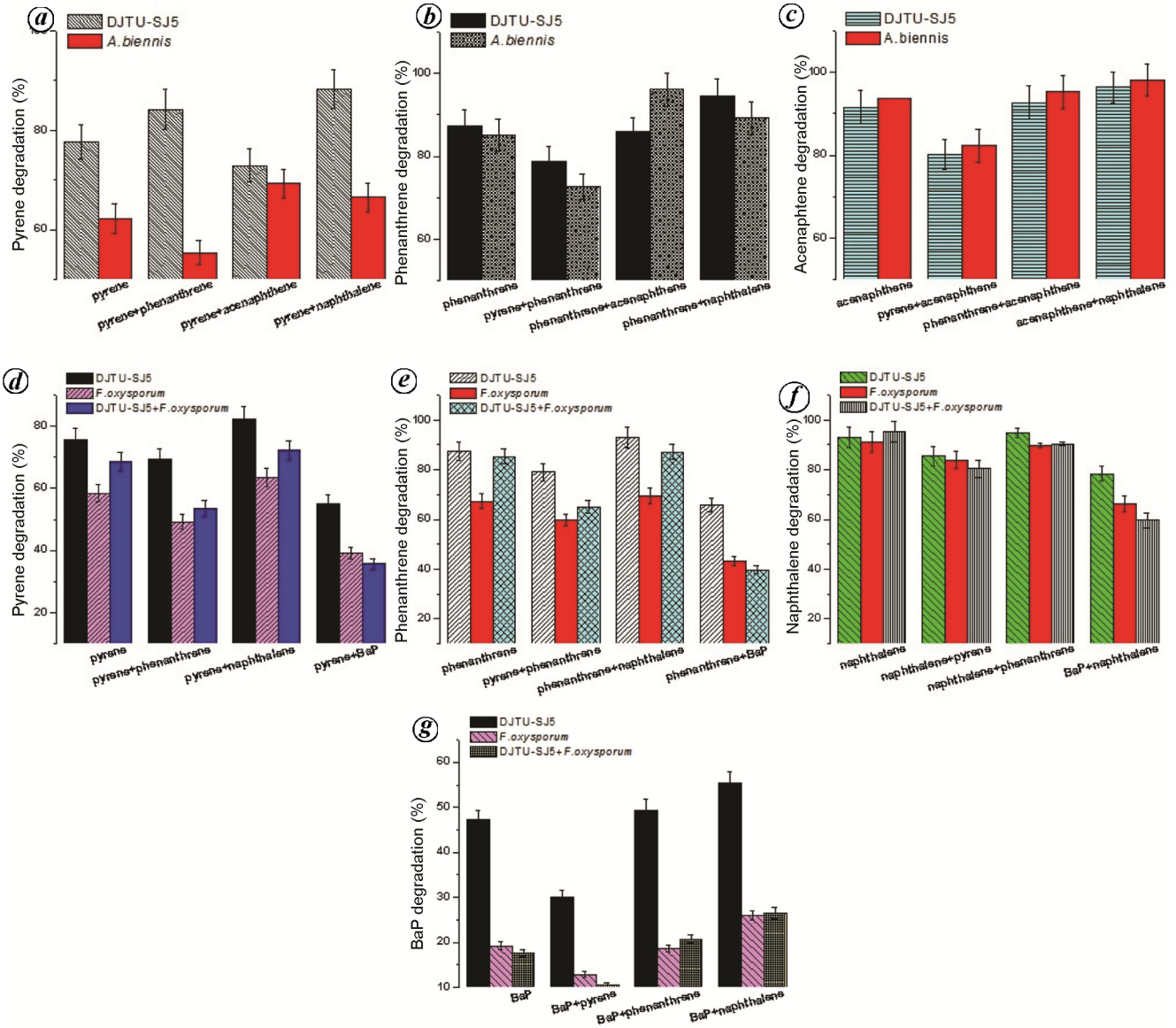

Figure 2. Twenty-four hour PAH degradation in single and/or binary substrate systems (***a*–*g***), and by fungal consortia (***d*–*g***). The final concentration of pyrene, phenanthrene, naphthalene, acenaphthene and benzopyrene was 95, 150, 200, 200 and 20 mg/l respectively. Error bars are standard deviations ($n = 3$).

bacteria and *F. oxysporum*. However, no significant co-operation between DJTU-SJ5 and F. oxysporum was observed in the present study. The high concentration of total PAHs might also be involved in the mitigation of fungal activity.

On the other hand, a few cases of co-metabolism were observed. For instance, naphthalene significantly stimulated the pyrene degradation of DJTU-SJ5 (Figure 2 *a*), while acenaphthene dramatically increased phenanthrene deprivation of *A. biennis* (Figure 2 *b*). The biostimulation of high molecular weight PAH degradation by naphthalene metabolite salicylate, a water-soluble and non-toxic degradation product, is useful for *in situ* bioremediation[17]. Both co-metabolism and competitive inhibition might be strain-specific. For example, naphthalene did not significantly enhance the phenanthrene degradation of *F. oxysporum* (Figure 2 *e*), while BaP inhibition of naphthalene degradation was more significant in *F. oxysporum* than in DJTU-SJ5 (Figure 2 *f*). Among the five PAHs, BaP was the most recalcitrant (Figures 1 and 2 *g*). Pyrene substantially decreased BaP degradation, especially in DJTU-SJ5, whereas phenanthrene failed to enhance its degradation via the single strain or the two-member consortium (Figure 2 *g*). Naphthalene, however, slightly increased BaP removal via the single strain or the consortium. *F. oxysporum* was recognized as a low BaP degrader[18]. Naphthalene, as the more easily degraded substrate, provided more carbon source, or cross acclimation might enhance the rate of biodegradation. These results provide potential in research for development of more diverse PAH removal methods and selectivity.

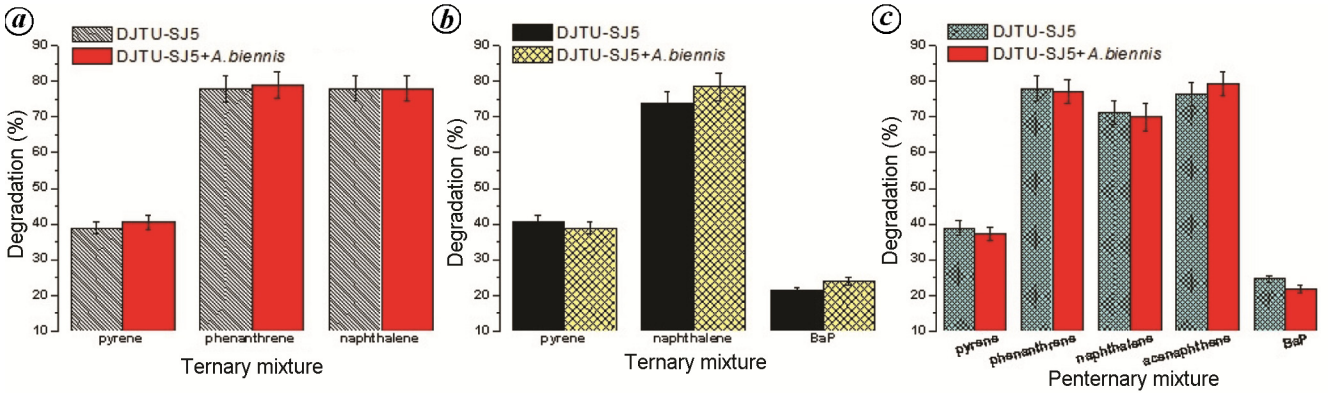

Figure 3. DJTU-SJ5/consortium-mediated mixed PAH degradation. ***a***, Five-day degradation of the ternary mixture consisting of 50 mg/l pyrene, 100 mg/l phenanthrene and 10 0mg/l naphthalene. ***b***, Five-day degradation of the ternary mixture consisting of 50 mg/l pyrene, 100 mg/l naphthalene and 100 mg/l pyrene and benzo[a]pyrene. ***c***, Five-day degradation of the penternary mixture consisting of 50 mg/l pyrene and 100 mg/l of naphthalene, acenaphthene, phenanthrene and BaP respectively. Error bars are standard deviations (n = 3).

Three or five PAHs were mixed together, which simulated the industrially produced effluent. The 5-d degradation efficiency of DJTU-SJ5 alone was comparable to that of the consortium (Figure 3 *a*–*c*), irrespective of the PAH mixture. The initial COD value was above 60,000 mg/l, which could be processed by DJTU-SJ5/consortium and was one order higher magnitude than that processed by a fungal consortium[19].

Chromatography and spectroscopy

After 7 d degradation in the culture of DJTU-SJ5, one major metabolite (retention time 10.904 min) of 100 mg/l pyrene (14.654 min) was detected (figure not shown). The lower degradation might be due to the toxicity of high concentration pyrene. In 150 mg/l phenanthrene degradation, the substrate (13.641 min) was reduced substantially. No substrate peak (9.384 min) was found in 200 mg/l naphthalene degradation. These results suggest nearly complete removal of phenanthrene/naphthalene via DJTU-SJ5. A product peak at 6.306 min was detected in 200 mg/l acenaphthene (12.401 min) degradation, while the substrate was decreased dramatically, suggesting the highly efficient removal of acenaphthene via DJTU-SJ5. Carboxylic acid, salicylic acid and phthalic acid were common metabolites of PAHs in fungal degradation[1]. Besides biotransformation, some studies suggest adsorption as one of the initial phases of subsequent transformation by fungi[20,21]. This would also partially explain the lack of metabolic intermediates.

After 72 h degradation of DJTU-SJ5, three major metabolites of BaP (9.944 min) were detected at 6.009, 8.097 min and 9.601 min respectively (figure not shown). Metabolite 1 had four major fragment ions, i.e. m/z 83, 122, 279 and 280. The m/z 122 might represent benzoic acid[22], while 280 might be BaP plus –CHO. Metabolite 2 had six major fragment ions, i.e. m/z 136, 150, 334, 406, 422 and 466. The m/z 136 and 150 might represent m-methylbenzoic acid and 2-ethyl benzoic acid respectively. The m/z, 334 might be BaP plus $–CHCH_2$ and –COCHO, m/z 406 might be 334 plus –COOH and –CHO, m/z 422 might be 406 plus –OH, whereas m/z 466 might be 422 plus –COOH. Metabolite 3 had one fragment ion of m/z 339, which might be BaP plus –OH and –CHCHCOOH. It is considered that the hydroxylation can be catalysed by cytochrome p450s (CYPs) and the hydroxylated carboxylic acid might be a major ring-cleavage metabolite of high molecular weight PAHs[17]. Both intracellular CYPs and extracellular peroxidases participate in the degradation of PAHs. The extracellular peroxidases might be important for the transformation of high molecular weight PAHs, since the latter could find it more difficult to penetrate through the cell membrane.

Transcriptome profiling

The illumina paired-end sequencing generated 50,128,308 (ordi), 45,047,260 (phen) and 44,118,522 (pyre) clean reads with 19,968,884,638 base pairs (19.9 Gb). Trinity assembled 33,084 unigenes (45,739 transcripts), corresponding to 41.88 Mb. The unigenes was 1266 bp (201–18,407 bp) long and N50 was 2135 bp. A total of 39860 ORFs were predicted. NR, Swissprot, String, GO, COG/KOG/NOG, Pfam and KEGG annotations were applicable for 77.3%, 40.9%, 26.0%, 49.0%, 40.9%, 43.6% and 36.2% of unigenes respectively.

In level-four GO annotation of biological process, 14.8% (4883) of unigenes fell under ‘organic cyclic compound metabolic process’ (Figure 4 *a*), followed by ‘cellular aromatic compound metabolic process’ (14.2%), ‘organic substance biosynthetic process’ (12.7%), etc. In level-three GO annotation of molecular function, 17.1% (5670) of unigenes fell under ‘organic cyclic compound binding’ (Figure 4 *b*), followed by ‘hydrolase activity’ (10.1%), ‘transferase activity’ (7.8%), ‘oxidoreductase activity’ (6.9%), ‘sequence-specific DNA binding

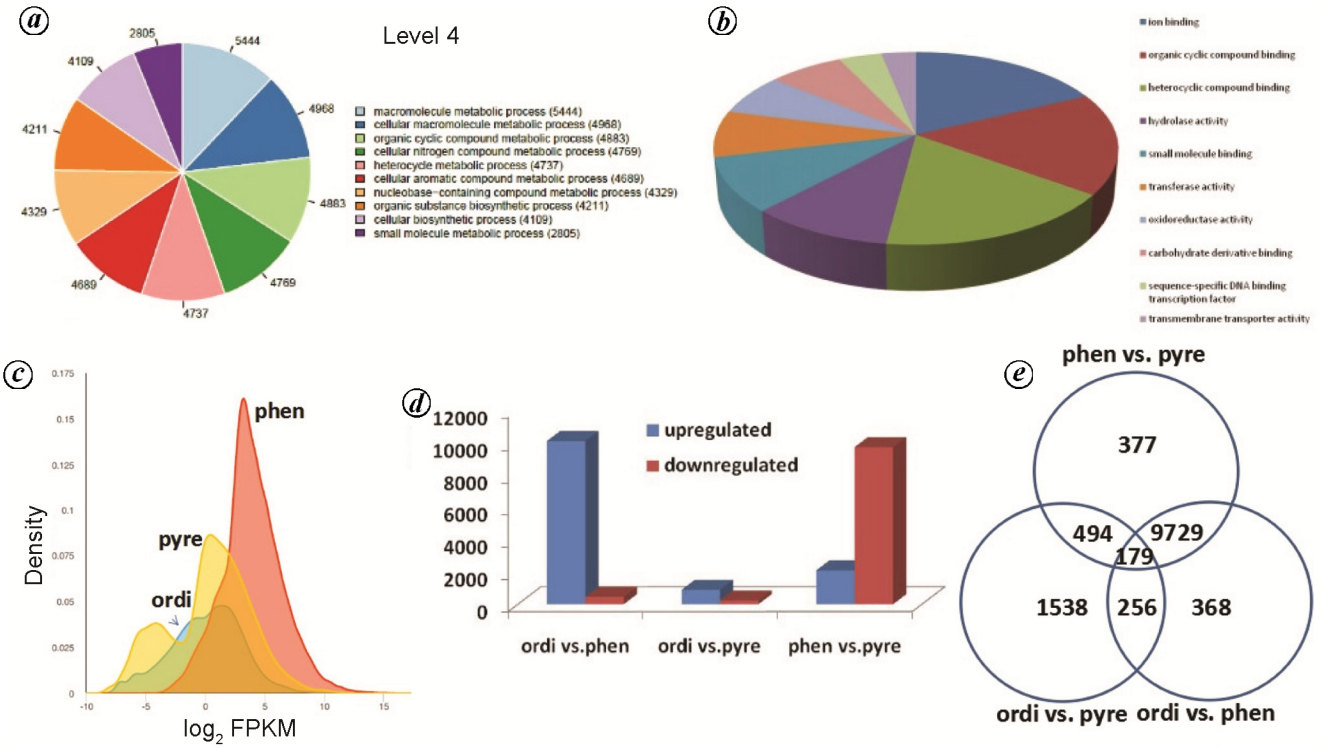

Figure 4. ***a***, Level-four GO annotation of biological process. ***b***, Level-three GO annotation of molecular function. ***c***, Expression density distribution of unigenes. ***d***, Number of differentially expressed genes (DEGs) in three comparisons. In a pairwise comparison, the former is control and the latter is treatment. ***e***, Common and unique DEGs in the three comparisons.

transcription factor' (4.0%) and 'transmembrane transporter activity' (3.2%). Many unigenes participating in the PAH transformation fell under the above GO terms. In COG/KOG annotation, 5.3% and 1.3% of unigenes fell under into 'secondary metabolite biosynthesis, transport and catabolism' and 'defence mechanisms' respectively.

In KEGG analysis, 1520 unigenes (4.6% of annotated genes) fell under 'biosynthesis of secondary metabolites' and 1017 under 'microbial metabolism in diverse environments'. Also, 109 unigenes belonged to 'degradation of aromatic compounds', followed by 'Metabolism of xenobiotics by CYP' (104), 'naphthalene degradation' (76) and 'PAH degradation' (59). Forty-nine, 33 and 24 unigenes fell under into 'ABC transporters', 'benzoate degradation' and 'toluene degradation' respectively. Unigenes belonging to 'bisphenol degradation' (17) and 'ethylbenzene degradation' (7) were also present in *Talaromyces verruculosus* transcriptomes. The statistics suggests great potential of the *Talaromyces* strain in PAH degradation.

In ordi sample, 97.3% clean reads were mapped to the *de novo*-assembled unigenes, and 91.5% and 91.9% reads were mapped to unigenes of phen and pyre respectively. A total of 11,528, 26,099 and 20,984 unigenes were expressed in ordi, phen and pyre respectively, suggesting the wide-ranging, elicitor-specific transcriptome reshaping. In terms of the unigene expression density distribution (Figure 4 *c*), there was one most concentrated area of gene expression in phen, in which the expression level was higher than that in the corresponding peak areas of ordi and pyre. The double peak areas of pyre, especially that of around $\log_2$FPKM-5 (very low gene expression), suggested that 100 mg/l pyrene was cytotoxic to the fungal strain and might be able to downregulate the mRNA expression of many genes. These results indicate histrionic transcriptome reshaping and reprogramming in *Talaromyces verruculosus* after PAH treatment.

Differentially expressed genes

A total of 10,532, 1,104 and 11,779 unigenes were differentially expressed between ordi and phen, ordi and pyre, and phen and pyre respectively (Figure 4 *d*). In total 368, 1538 and 377 DEGs were solely found between ordi and phen, ordi and pyre, and phen and pyre respectively (Figure 4 *e*). For DEGs, $\log_2$FC of ordi expression versus phen expression varied from –10.63 to 17.45. The $\log_2$FC of ordi versus pyre and phen versus pyre ranged between –10.63 and 12.65, and –15.97 and 11.35 respectively. This indicates that 100 mg/l phenanthrene elicited stronger and more widespread responses in the gene expression of *T. verruculosus* than 100 mg/l pyrene.

Functionally related genes tend to have analogous expression patterns. In the cluster analysis, 12,578 DEGs belonged to 10 unique clusters in the union set of ordi versus phen, ordi versus pyre and phen versus pyre. The

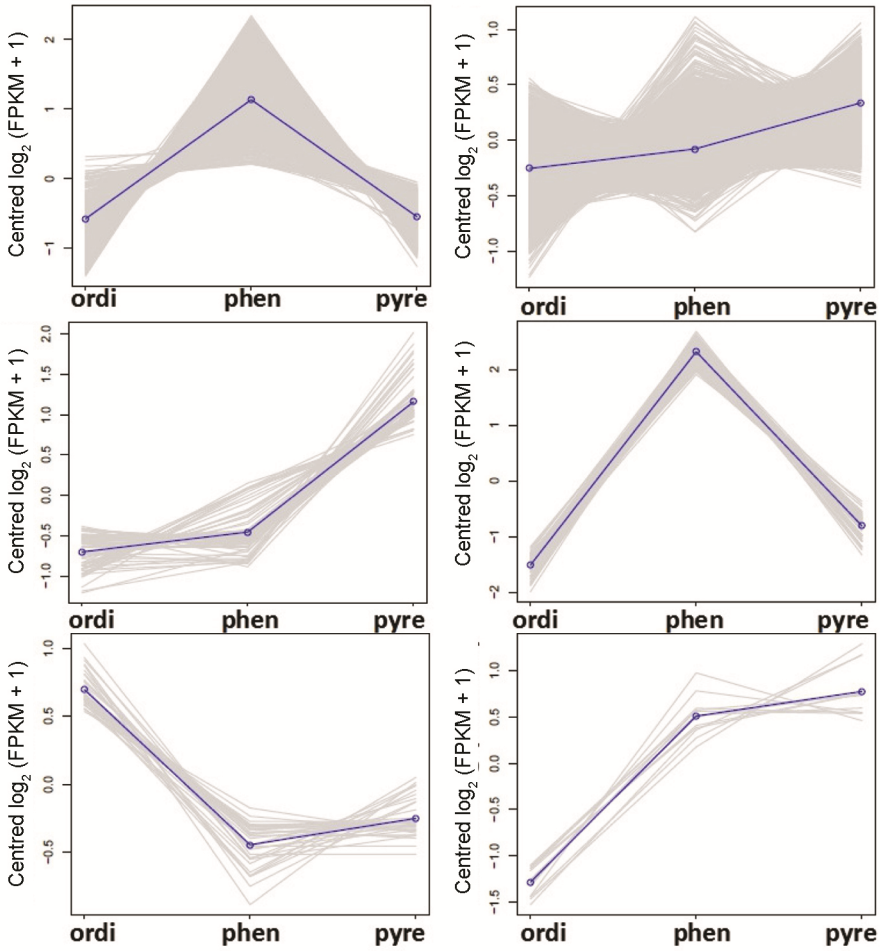

Figure 5. Trend lines showing DEG expression levels of six major clusters. A total of 12,578 DEGs fall into 10 unique clusters showing distinct expression patterns in the union set of ordi versus phen, ordi versus pyre, and phen versus pyre. Each line represents a unigene, and the line with hollow circles represents the average expression value of all unigenes in the same cluster. Each of clusters 5 and 8–10 has no more than two unigenes, and is not shown.

largest was cluster one, consisting of 9642 unigenes. These genes had the highest expression in phen (centred $\log_2(\text{FPKM} + 1) = 1.131 \pm 0.372$) (Figure 5), and their expression levels were comparable in ordi and pyre (–0.580 versus –0.550). Cluster two was the second largest, consisting of 2733 unigenes. These genes were upregulated in phen (–0.079 versus ordi –0.256) and continued to be upregulated under pyrene treatment (0.336). Many genes of this cluster participated in PAH degradation and detoxification, as well as stress and defence reactions.

The initial steps of PAH transformation in many filamentous fungi involved CYPs and epoxide hydrolases (Figure 6). The metabolic intermediates of high molecular weight PAHs, could be more easily internalized to be transformed by intracellular CYPs and other enzymes. There were 25 CYPs in cluster two, including those responsible for the formation of epoxide and other oxidative products. Epoxide hydrolase c13299_g1 was upregulated in both pyre (0.488) and phen (0.147), while c11627_g1, also representing this enzyme, was solely increased in pyre (0.344). Benzoate 4-monooxygenases (c13234_g2 and c26147_g1) were upregulated in phen (0.408 and –0.069 respectively) and pyre (0.050 and 0.211 respectively) when compared with ordi (–0.459 and –0.141 respectively). Six alkane-inducible CYPs, belonging to the CYP52 subfamily, suggested that *T. verruculosus* CYP-dependently converted alkanes to fatty acids[23], which could be beneficial in maintaining the membrane integrity under stress conditions. In addition, eight flavin containing monooxygenases (FMOs) were upregulated in cluster two.

The eukaryotic microsomal CYP systems consist of a CYP and a CYP redox partner, which is a CYP reductase (CPR) that donates electrons from NADPH[24]. However, CPR c15580_g1 was downregulated in both pyre (0.033 versus 0.134 of ordi) and phen (–0.167). Other electron donors might be present in *Talaromyces*. Cytochrome b5 reductase (c12343_g1 and c10741_g1), NADH-dependent and attached to the endoplasmic reticulum, was substantially upregulated in phen (1.019 and 0.723

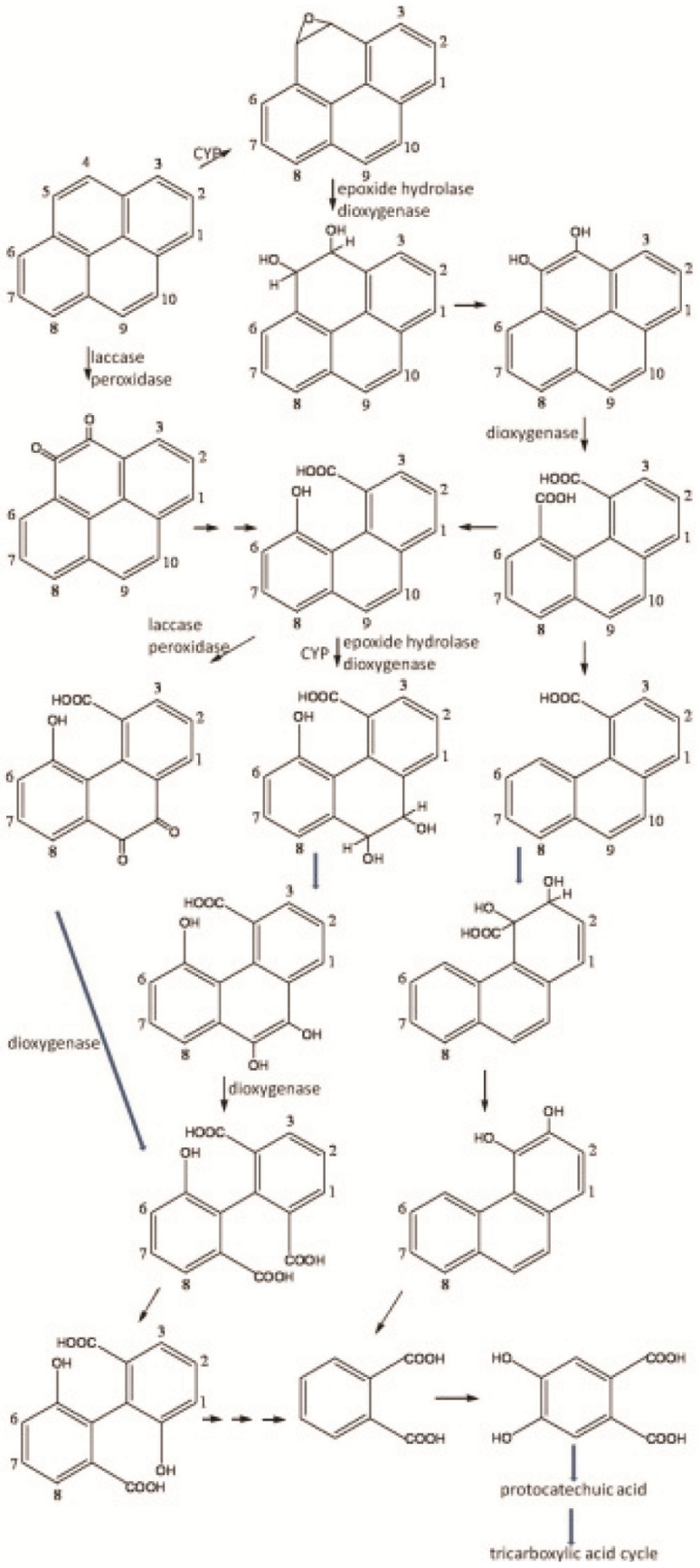

Figure 6. Proposed pathways of pyrene degradation in *Talaromyces verruculosus*.

respectively) and pyre (0.194 and 0.169 respectively), suggesting their essential role in PAH oxidation and electron transfer.

In a comparative metatranscriptomics study, the addition of phenanthrene caused a 1.8–33-fold increase in the amount of dioxygenase[25], and most dioxygenase transcripts were generated by actinobacteria. Naphthalene dioxygenase[26], PAH-ring hydroxylating dioxygenase (RHD)[27], and catechol 1,2-dioxygenase[28] participated in the bacterial transformation of pyrene and other high molecular weight PAHs. Some *Trichoderma* species were potent aromatic hydrocarbon-degrading fungi[29], which used multicopper laccases, peroxidases and ring-cleavage dioxygenases in metabolizing low and high molecular weight PAHs. So far, no PAH degrading dioxygenase has been reported in *Talaromyces*. In the present study, 30 dioxygenase unigenes were found to be expressed in cluster two of the *Talaromyces* strain. For instance, PAH-RHDc11562_g1 and aromatic ring-opening dioxygenasec10451_g1 were significantly upregulated in pyre, participating in the oxidation and opening of the aromatic rings. The mRNA expression of catechol 1,2-dioxygenase (unigenesc 12691_g1 and c11759_g1) was upregulated in phenanthrene-treated fungi (–0.267 versus –0.438 and –0.068 versus –0.416 respectively) when compared with ordi, and the upregulation was more obvious in pyrene-treated fungi (0.705 and 0.485 respectively). Salicylate hydroxylase (c17847_g1), at the upstream of catechol dioxygenase along the phenanthrene degradation pathway of *Trichoderma*[29], was significantly upregulated in pyre (0.195 versus –0.097) rather than in phen (–0.097). Salicylic acid and catechol might be intermediaries in the degradation of both phenanthrene and pyrene. Tyrosinase (c21755_g1) carried out the oxidation of catechol to form benzoquinone. Carboxy-cis, cis-muconate might be at the downstream of catechol and can be converted to lactone via the catalysis of carboxy-cis,cis-muconate cyclase (c18907_g1; lactonase). The β-ketoadipate pathway in soil-borne fungi was found essential to destroy phenolics in root exudate and inside the roots for their robustness[30]. Homogentisate 1,2-dioxygenase (c11287_g1), implicated in the fungal dilapidation of aromatic dye[31], was solely upregulated in pyre (0.918 versus –0.432 of ordi and –0.485 of phen). The unigene c24097_g1, similar to the protocatechuate dioxygenase, was upregulated in pyre (0.170 versus –0.085 of ordi). Bacterial protocatechuate dioxygenases catalyse the ring cleavage of aromatic acid derivatives[32,33]. The present study detected both protocatechuate dioxygenase and catechol 1,2-dioxygenase in *Talaromyces*, indicating that fungi could utilize the β-ketoadipate pathway to degrade pyrene and relevant aromatics. There are complex interactions between prokaryotes and eukaryotes in the rhizosphere, and horizontal gene transfer is possible to share the degradation traits between two taxonomic groups.

Dehydrogenases are useful to transform dihydrodiols to the hydroxylated intermediates. One hundred eighty-four unigenes of cluster two represented various dehydrogenases. Aldehyde and semialdehyde were common intermediates in degrading PAHs[29,34]. Twenty aldehyde/semialdehyde dehydrogenases were induced in response to pyrene or both pyrene and phenanthrene, which might be essential in utilizing the non-native substrate as a carbon source[35]. In *Bacillus*, semialdehyde was converted from protocatechuate via dioxygenase catalysis[34], which can be converted to carboxylic acid via dehydrogenase catalysis. The upregulated semialdehyde dehydrogenases (c5422_g1, c7813_g1 and c7151_g1) suggest the presence of this pathway in *Talaromyces*. Aldolase was required by the last step of the protocatechuate 4,5-cleavage pathway[36]. Nine aldolase unigenes were upregulated in pyre or both phen and pyre. Significantly upregulated expression of four lactate dehydrogenase unigenes (c14243_g1, c12855_g1, c19912_g1 and c16621_g1) in pyre, or both pyre and phen implies enhancement of PAH mineralization via TCA cycle.

A *Mycobacterium vanbaalenii* strain produced the O-methylated derivatives of non-K-region phenanthrene- and pyrene-diols during degradation[37]. Interestingly, eight *O*-methyltransferases (OMTs) were upregulated in pyre, phen, or both. For example, the expression of catechol OMT c8020_g1 was higher in phen (0.040) than in ordi (–0.463), and it was further enhanced in pyre (0.423). Caffeic acid 3-OMT c13884_g1 was enriched in phen (0.530) and pyre (0.346). These data suggest the presence of methylation pathway in fungal degradation.

The products of reactions catalysed by oxygenases may comprise phenols, trans-dihydrodiols, quinones and dihydrodiolepoxides, which may convert to glucosides, glucuronides, xylosides and sulphates[29]. In cluster two, a UDP-glucosyl transferase family protein gene (c11967_g1) was upregulated in phen (0.337) and pyre (0.136) when compared with ordi (–0.474). An arylsulphotransferase (c12889_g1) was upregulated in pyre (0.355) and phen (–0.040) when compared with ordi (–0.315). These enzymes are functionally similar to the mammalian phase II xenobiotic metabolizing enzymes[38], which might be essential in the detoxification of PAHs and their degradation products.

Three multicopper oxidases (laccase; c11106_g2, c11944_g1, and c10949_g1) and three peroxidases (c6093_g1, c15960_g1, and c16607_g1) were upregulated in pyre, or both pyre and phen. These enzymes offered advantages for the utilization of naturally occurring aromatic compounds (e.g. lignin derivatives) and improved fungal survival in soils, and were essential for PAH degradation. The catalase (c9791_g1 and c15782_g1) activity might also be involved in the mineralization of pyrene in soil[39].

Conclusion

This study showed that PAH-degrading fungi isolated from *Taxus* rhizosphere showed favourable biotransformation

activities. The statistically based experimental designs are well suited for optimizing the PAH-degrading medium composition. In some PAH-polluted sites, the soil is too acidic or alkaline. Such conditions are not conducive to fungal activity, thereby reducing the biodegradation of PAHs. The addition of chemicals could adjust the pH at those sites, in order to foster an environment for effective biodegradation[20]. DJTU-SJ5 and DJTU-SJ5-containing consortium proved to be most efficient in PAH degradation, which was confirmed by spectral and chromatographic analyses. The DJTU-SJ5-containing fungal consortium lends the potential for use in an industrial setting. The intracellular enzymes might be the major factor in PAH removal, which was supported by the Illumina transcriptome sequencing of *Talaromyces* strains with/without PAH attack, as well as the transcriptome characterization. Multiple fungal enzymes with oxidizing and reducing capacities might participate in the biotransformation and degradation of PAHs. Further studies of enzyme characterization and process optimization at the bench level and industrial scale are warranted. PAHs could be subjected to volatilization, adsorption, photolysis and chemical oxidation, but it is well known that the microbial transformation is the major detoxification process[20]. Indeed, studies of PAH adsorption to the fungal biomass are necessary.

1. Haritash, A. K. and Kaushik, C. P., Biodegradation aspects of polycyclic aromatic hydrocarbons (PAHs): a review. *J. Hazard. Mater*., 2009, **169**, 1–15.
2. Hao, D. C., Zhang, C. R. and Xiao, P. G., The first Taxus rhizosphere microbiome revealed by shotgun metagenomic sequencing. *J. Basic Microbiol.*, 2018, **58**, 501–512.
3. Goyari, S., Devi, S. H., Bengyella, L., Khan, M. and Sharma, C. K., Unveiling the optimal parameters for cellulolytic characteristics of *Talaromyces verruculosus* SGMNPf3 and its secretory enzymes. *J. Appl. Microbiol*., 2015, **119**, 88–98.
4. Fang, D. and Shi, C., Characterization and flocculability of a novel proteoglycan produced by *Talaromyces trachyspermus* OU5. *J. Biosci. Bioeng*., 2016, **121**, 52–56.
5. Aggelis, G., Ehaliotis, C., Nerud, F., Stoychev, I. and Lyberatos, G., Evaluation of white-rot fungi for detoxification and decolorization of effluents from the green olive debittering process. *Appl. Microbiol. Biotechnol*., 2002, **59**, 353–360.
6. Jarosz-Wilkołazka, A., Graz, M., Braha, B., Menge, S. and Schlosser, D., Species-specific Cd-stress response in the white rot basidiomycetes *Abortiporus biennis* and *Cerrena unicolor*. *Biometals*, 2006, **19**, 39–49.
7. Koutrotsios, G. and Zervakis, G. I., Comparative examination of the olive mill wastewater biodegradation process by various wood-rot macrofungi. *Biomed. Res. Int*., 2014, **2014**, 482937.
8. Pasricha, S., Payne, M., Canovas, D., Pase, L. and Ngaosuwankul, N., Cell-type-specific transcriptional profiles of the dimorphic pathogen *Penicillium marneffei* reflect distinct reproductive, morphological, and environmental demands. *G3*, 2013, **3**, 1997–2014.
9. Lau, S. K. P., Tsang, C. C. and Woo, P. C. Y., *Talaromyces marneffei* genomic, transcriptomic, proteomic and metabolomics studies reveal mechanisms for environmental adaptations and virulence. *Toxins*, 2017, **9**, pii: E192.
10. Hao, D. C., Ge, G. B. and Yang, L., Bacterial diversity of *Taxus* rhizosphere: culture-independent and culture-dependent approaches. *FEMS Microbiol. Lett*., 2008, **284**, 204–212.
11. Dou, T. Y., Luan, H. W., Ge, G. B., Dong, M. M. and Zou, H. F., Functional and structural properties of a novel cellulosome-like multienzyme complex: efficient glycoside hydrolysis of water-insoluble 7-xylosyl-10-deacetylpaclitaxel. *Sci. Rep*., 2015, **5**, 13768.
12. Hao, D. C., Chen, S. L., Osbourn, A., Kontogianni, V. G. and Liu, L. W., Temporal transcriptome changes induced by methyl jasmonate in *Salvia sclarea*. *Gene*, 2015, **558**, 41–53.
13. Hao, D. C., Song, S. M., Mu, J., Hu, W. L. and Xiao, P. G., Unearthing microbial diversity of *Taxus* rhizosphere via MiSeq high-throughput amplicon sequencing and isolate characterization. *Sci. Rep*., 2016, **6**, 22006.
14. Wang, J., Li, F., Li, X., Wang, X. and Li, X., Effects of electrokinetic operation mode on removal of polycyclic aromatic hydrocarbons (PAHs), and the indigenous fungal community in PAH-contaminated soil. *J. Environ. Sci. Health A*, 2013, **48**, 1677–1684.
15. Polak, J. and Jarosz-Wilkołazka, A., Whole-cell fungal transformation of precursors into dyes. *Microb. Cell Fact*., 2010, **9**, 51.
16. Jacques, R. J., Okeke, B. C., Bento, F. M., Teixeira, A. S. and Peralba, M. C., Microbial consortium bioaugmentation of a polycyclic aromatic hydrocarbons contaminated soil. *Bioresour. Technol*., 2008, **99**, 2637–2643.
17. Rentz, J. A., Alvarez, P. J. and Schnoor, J. L., Benzo[a]pyrene degradation by *Sphingomonas yanoikuyae* JAR02. *Environ. Pollut*., 2008, **151**, 669–677.
18. Verdin, A., Lounès-HadjSahraoui, A., Laruelle, F., Grandmougin-Ferjani, A. and Durand, R., Effect of the high polycyclic aromatic hydrocarbon, benzo[a]pyrene, on the lipid content of *Fusarium solani*. *Mycol. Res*., 2006, **110**, 479–484.
19. Gullotto, A., Lubello, C., Mannucci, A., Gori, R. and Munz, G., Biodegradation of naphthalene sulphonate polymers: the potential of a combined application of fungi and bacteria. *Environ. Technol*., 2015, **36**, 538–545.
20. Ghosal, D., Ghosh, S., Dutta, T. K. and Ahn, Y., Current state of knowledge in microbial degradation of polycyclic aromatic hydrocarbons (PAHs): a review. *Front. Microbiol*., 2016, **7**, 1369.
21. Batista-García, R. A., Kumar, V. V., Ariste, A., Tovar-Herrera, O. E. and Savary, O., Simple screening protocol for identification of potential mycoremediation tools for the elimination of polycyclic aromatic hydrocarbons and phenols from hyperalkalophile industrial effluents. *J. Environ. Manage*., 2017, **198**, 1–11.
22. Hadibarata, T. and Kristanti, R. A., Fate and cometabolic degradation of benzo[a]pyrene by white-rot fungus *Armillaria* sp. F022. *Bioresour. Technol*., 2012, **107**, 314–318.
23. Del Carratore, R., Gervasi, P. G., Contini, M. P., Beffy, P. and Maserti, B. E., Expression and characterization of two new alkane-inducible cytochrome P450s from *Trichoderma harzianum*. *Biotechnol. Lett*., 2011, **33**, 1201–1206.
24. Gutiérrez, M. S., Rojas, M. C., Sepúlveda, D., Baeza, M. and Cifuentes, V., Molecular characterization and functional analysis of cytochrome b5 reductase (CBR) encoding genes from the carotenogenic yeast *Xanthophyllomyces dendrorhous*. *PLoS ONE*, 2015, **10**, e140424.
25. de Menezes, A., Clipson, N. and Doyle, E., Comparative metatranscriptomics reveals widespread community responses during phenanthrene degradation in soil. *Environ. Microbiol*., 2012, **14**, 2577–2588.
26. Kumari, S., Regar, R. K., Bajaj, A., Ch, R. and Satyanarayana, G. N. V., Mudian, M. K. R. and Manickam, N., Simultaneous biodegradation of polyaromatic hydrocarbons by a *Stenotrophomonas* sp: characterization of nidgenes and effect of surfactants on degradation. *Indian J. Microbiol*., 2017, **57**, 60–67.
27. Muangchinda, C., Yamazoe, A., Polrit, D., Thoetkiattikul, H. and Mhuantong, W., Biodegradation of high concentrations of mixed polycyclic aromatic hydrocarbons by indigenous bacteria from a

river sediment: a microcosm study and bacterial community analysis. *Environ. Sci. Pollut. Res. Int*., 2017, **24**, 4591–4602.
28. Meena, S. S., Sharma, R. S., Gupta, P., Karmakar, S. and Aggarwal, K. K., Isolation and identification of *Bacillus megaterium* YB3 from an effluent contaminated site efficiently degrades pyrene. *J. Basic Microbiol*., 2016, **56**, 369–378.
29. Zafra, G. and Cortés-Espinosa, D. V., Biodegradation of polycyclic aromatic hydrocarbons by *Trichoderma* species: a mini review. *Environ. Sci. Pollut. Res. Int*., 2015, **22**, 19426–19433.
30. Michielse, C. B., Reijnen, L., Olivain, C., Alabouvette, C. and Rep, M., Degradation of aromatic compounds through the β-ketoadipate pathway is required for pathogenicity of the tomato wilt pathogen *Fusarium oxysporum* f. sp. Lycopersici. *Mol. Plant. Pathol*., 2012, **13**, 1089–1100.
31. Sun, S., Xie, S., Chen, H., Cheng, Y. and Shi, Y., Genomic and molecular mechanisms for efficient biodegradation of aromatic dye. *J. Hazard. Mater*., 2016, **302**, 286–295.
32. Guzik, U., Hupert-Kocurek, K., Sitnik, M. and Wojcieszyńska, D., Protocatechuate 3,4-dioxygenase: a wide substrate specificity enzyme isolated from *Stenotrophomonas maltophilia* KB2 as a useful tool in aromatic acid biodegradation. *J. Mol. Microbiol. Biotechnol*., 2014, **24**, 150–160.
33. Li, J., Luo, C., Song, M., Dai, Q. and Jiang, L., Biodegradation of phenanthrene in polycyclic aromatic hydrocarbon-contaminated wastewater revealed by coupling cultivation-dependent and independent approaches. *Environ. Sci. Technol*., 2017, **51**, 3391–3401.
34. Doddamani, H. P. and Ninnekar, H. Z., Biodegradation of phenanthrene by a *Bacillus* species. *Curr. Microbiol*., 2000, **41**, 11–14.
35. Aziz, R. K., Monk, J. M., Andrews, K. A., Nhan, J. and Khaw, V. L., The aldehyde dehydrogenase, AldA, is essential for L-1,2-propanediol utilization in laboratory-evolved *Escherichia coli*. *Microbiol. Res*., 2017, **194**, 47–52.
36. Ni, B., Zhang, Y., Chen, D. W., Wang, B. J. and Liu, S. J., Assimilation of aromatic compounds by *Comamonas testosteroni*: characterization and spreadability of protocatechuate 4,5-cleavage pathway in bacteria. *Appl. Microbiol. Biotechnol*., 2013, **97**, 6031–6041.
37. Kim, Y. H., Freeman, J. P., Moody, J. D., Engesser, K. H. and Cerniglia, C. E., Effects of pH on the degradation of phenanthrene and pyrene by *Mycobacterium vanbaalenii* PYR-1. *Appl. Microbiol. Biotechnol*., 2005, **67**, 275–285.
38. Hao, D. C., Xiao, P. G. and Chen, S. L., Phenotype prediction of nonsynonymous single nucleotide polymorphisms in human phase II drug/xenobiotic metabolizing enzymes: perspectives on molecular evolution. *Sci. China Life Sci*., 2010, **53**, 1252–1262.
39. Liu, T., Wei, L., Qiao, M., Zou, D. and Yang, X., Mineralization of pyrene induced by interaction between *Ochrobactrum* sp. PW and ryegrass in spiked soil. *Ecotoxicol. Environ. Saf*., 2016, **133**, 290–296.

ACKNOWLEDGEMENTS. The authors acknowledge the support from Conselho Nacional de DesenvolvimentoCientífico e Tecnológico Project number 477668/2012-7 and Mackenzie Presbyterian University, São Paulo, Brazil.

Received 30 June 2018; revised accepted 13 December 2018

doi: 10.18520/cs/v116/i7/1218-1228